Combined effect of damage and plastic anisotropy on the ductility limit of thin metal sheets

Sabeur MSOLLI[a,]*, Mohamed BEN BETTAIEB[a,b], Farid ABED-MERAIM[a,b]

[a]LEM3, UMR CNRS 7239 – Arts et Métiers ParisTech, 4 rue Augustin Fresnel, 57078 Metz Cedex 3, France
[b]DAMAS, Laboratory of Excellence on Design of Alloy Metals for low-mAss Structures, Université de Lorraine, France

Abstract

It is well known that both damage and plastic anisotropy strongly affect the ductility limit of thin metal sheets. Due to the manufacturing processes, initial defects, such as inclusions and voids, are commonly present in the produced sheet metals. Plastic anisotropy is a direct outcome of the rolling process, where the resulting metal sheets exhibit preferred crystallographic orientations or strong texture. In the present study, the combined effect of plastic anisotropy and damage on localized necking is numerically investigated and analyzed. To this aim, an improved version of the Gurson−Tvergaard−Needleman (GTN) constitutive framework is used to model the mechanical behavior of the studied sheet. This version, which is an extension of the original GTN model, incorporates Hill's anisotropic yield function to take into account the plastic anisotropy of the matrix material. Particular attention is devoted to the derivation of the analytical tangent modulus associated with this constitutive model. This extended GTN model is successfully coupled with bifurcation theory to predict sheet metal ductility limits, which are represented in terms of forming limit diagrams (FLDs). The effect of some material parameters (e.g., anisotropy parameters of the metallic matrix) on the shape and the location of the predicted FLDs is then investigated and discussed through numerical simulations.

Keywords: damage; anisotropy; ductility limit; bifurcation; GTN model

* Corresponding author. Tel.: +33 3 87 37 54 79; fax: +33 3 87 37 54 70.
 E-mail address: sabeur.msolli@ensam.eu

1. Introduction

Sheet metal forming is one of the most used processes in manufacturing industries. This process involves plastic deformation of metallic sheets and is designed to obtain complex parts with fast cadence. Nevertheless, it happens that localized necking occurs in the drawn part before the end of forming operations. The onset of this localized necking represents the ultimate deformation that the drawn part can undergo, since this phenomenon is often precursor to material failure. Hence, efficient and reliable prediction of the occurrence of localized necking is required to help in the calibration of the process controlling parameters. The most common representation for the necking limit strains relies on the concept of forming limit diagram (FLD), which was initially proposed by Keeler and Backofen (1963). The prediction of such diagrams requires the combination of a plastic instability criterion and a constitutive model that describes the mechanical behavior of the studied sheet. Our attention in this paper is focused on materials exhibiting plastic anisotropy. Such anisotropic behavior is due to rolling operations, which are performed before the forming process. It is expected that plastic anisotropy plays a crucial role in the prediction of localized necking in sheet metals. Hence, accurate predictions of strain localization are needed, especially for anisotropic materials and for complex loading paths. The onset of localized necking may occur as a bifurcation from a homogeneous deformation state or it may be triggered by some assumed initial imperfection. Accordingly, two main classes of strain localization criteria can be found in the literature:

- Imperfection approach: This approach has been initially developed by Marciniak and Kuczynski (1967). It is based on the assumption that an initial imperfection exists in the form of a narrow band across the section of the studied sheet. This approach, denoted hereafter as M–K approach, has been first applied to rigid-plastic materials following the von Mises isotropic yield function. Then, the M–K approach has been extended to take into account the plastic anisotropy of the metal sheets, by considering different formulations for the adopted yield functions. In this context, one can quote the work of Butuc et al. (2002), who used the Barlat yield function (Barlat, 1987), Cao et al. (2000), who used the Karafillis and Boyce yield function (Karafillis and Boyce, 1993), and Kim et al. (2003), who used the YLD 2000. In spite of the over-sensitivity of its predictions to the initial imperfection value, the M–K approach has attracted a great deal of attention in both academic and industrial applications, due to its pragmatic character.

- Bifurcation theory: In addition to its sound mathematical foundations, the bifurcation theory does not require any fitting parameter, such as the initial imperfection needed in the M–K analysis. This theory has been initially applied by Hill (1952) to materials obeying flow theory of plasticity. In the latter case, both hardening and plasticity were assumed to be isotropic. To predict ductility limits at realistic strain levels for the whole range of strain paths (i.e., from the uniaxial tensile state to equibiaxial tension), the bifurcation approach must be combined with constitutive models exhibiting some destabilizing effects. The development of such destabilizing effects may be due to the application of the deformation theory of plasticity (see, e.g., Stören and Rice, 1975), or the use of the Schmid law within the framework of crystal plasticity (see, e.g., Franz et al., 2013). This destabilizing effect may also be due to some softening behavior introduced in the constitutive modeling through coupling with damage (Mansouri et al., 2014). To account for the effect of plastic anisotropy on localized necking predictions, the constitutive models are usually coupled with anisotropic yield criteria. In this field, one can quote Hill'48 yield function, which has been coupled with the deformation theory of plasticity in Jaamialahmadi and Kadkhodayan (2011), and with the Lemaitre damage model in Haddag et al. (2009). This coupling allows analyzing the effect of plastic anisotropy on the shape and the level of FLDs predicted by bifurcation theory. The main objective of the present contribution is to expand these earlier investigations by coupling an improved version of the Gurson–Tvergaard–Needleman (GTN) damage model with the bifurcation theory. This improved version extends the original one to take into account the plastic anisotropy of the matrix material. The Hill'48 yield function is used to model this plastic anisotropy.

The present paper is organized as follows:
- In Section 2, the constitutive equations describing the improved GTN model are presented.
- Section 3 details the coupling between the bifurcation theory and the improved GTN model.

- The various numerical predictions are presented in Section 4.

Nomenclature

K, ε_0, n	Swift's hardening parameters of the dense matrix
$\bar{\varepsilon}^p$	equivalent plastic strain of the dense matrix
$\bar{\sigma}$	flow stress of the dense matrix
$\boldsymbol{D}^p$	macroscopic plastic strain rate tensor (dense matrix+voids)
$\dot{\gamma}$	plastic multiplier
$\boldsymbol{\Sigma}$	macroscopic Cauchy stress tensor
F,G,H,L,M,N	Hill's matrix components
$\boldsymbol{H}$	Hill's anisotropy matrix
r_0, r_{45}, r_{90}	Lankford's coefficients
q	anisotropic equivalent stress
Σ_m	hydrostatic part of the macroscopic stress $\boldsymbol{\Sigma}$
q_1, q_2, q_3	damage constants
Φ_{GTN}	yield function of the improved GTN model
f	total void volume fraction (also called porosity)
f_c	critical void volume fraction
f_F	final void volume fraction
f_g	volume fraction of grown voids
f_n	volume fraction of nucleated voids
f_N	volume fraction of inclusions tending to nucleate
f_u	ultimate void volume fraction
f^*	modified volume fraction of voids
ε_N	equivalent plastic strain for which half of inclusions have nucleated
s_N	standard deviation on ε_N
$\boldsymbol{C}^e$	fourth-order elasticity tensor
$\boldsymbol{C}^{ep}$	elastic-plastic tangent modulus
$\boldsymbol{L}$	analytical tangent modulus
$\boldsymbol{I}$	second-order identity tensor

---

2. Constitutive equations

In this work an improved GTN model is used to take into account the plastic anisotropy of the matrix. In addition to the classical equations that are common to conventional elastic-plastic constitutive models (i.e., decomposition of the deformation into elastic and plastic parts, hypo-elastic law…), the current version of GTN model is defined by the following supplementary equations:

- The expression of the yield function:

$$\Phi_{GTN} = \left(\frac{q}{\bar{\sigma}}\right)^2 + 2\,q_1\,f^*cosh\left(\frac{3\,q_2\,\Sigma_m}{\kappa\bar{\sigma}}\right) - 1 - q_3\,f^{*2}, \tag{1}$$

where q and Σ_m are equal to $\sqrt{\Sigma : \boldsymbol{H} : \Sigma / 2}$ and $\mathrm{tr}(\Sigma)/3$, respectively, while κ is a coefficient reflecting the plastic anisotropy effect and which depends on r_0, r_{45} and r_{90} through coefficients h_i (Benzerga and Besson, 2001):

$$\kappa = \sqrt{1.6\left(\frac{h_1 + h_2 + h_3}{h_1 h_2 + h_2 h_3 + h_1 h_3}\right) + 0.8\left(\frac{1}{h_4} + \frac{1}{h_5} + \frac{1}{h_6}\right)}. \tag{2}$$

The matrix $\boldsymbol{H}$ used to compute the anisotropic equivalent stress q is expressed by the following relation:

$$\boldsymbol{H} = \begin{bmatrix} G+H & -H & -G & 0 & 0 & 0 \\ -H & H+F & -F & 0 & 0 & 0 \\ -G & -F & F+G & 0 & 0 & 0 \\ 0 & 0 & 0 & 2N & 0 & 0 \\ 0 & 0 & 0 & 0 & 2L & 0 \\ 0 & 0 & 0 & 0 & 0 & 2M \end{bmatrix}. \tag{3}$$

The components F, G, H, L, M and N are related to the r_0, r_{45} and r_{90} coefficients by the following relations:

$$F = \frac{H}{r_{90}}; \quad G = \frac{H}{r_0}; \quad H = \frac{r_0}{r_0 + 1}; \quad L = M = \frac{3}{2}; \quad N = \frac{(r_0 + r_{90})(2r_{45} + 1)}{2r_{90}(r_0 + 1)}. \tag{4}$$

As demonstrated by Eq. (1), the yield surface strongly depends on the plastic anisotropy of the matrix material. This dependency is reflected by the introduction of Hill's matrix $\boldsymbol{H}$ into the expression of the equivalent stress q, on the one hand, and by the introduction of the scalar parameter κ into the '$cosh$', on the other hand. It must be noted that when coefficients r_0, r_{45} and r_{90} are equal to 1 (case of isotropic materials), the classical GTN yield surface is obviously recovered. Indeed, in this particular case, the scalar functions q and κ become equal to $\sqrt{(3/2)\Sigma_d : \Sigma_d}$ (Σ_d being the deviatoric part of Σ) and 2, respectively.

The expression of f^* is given by the empirical formula introduced in Tvergaard and Needleman (1984).

- The evolution of void volume fraction: the porosity rate $\dot{f}$ is additively decomposed into nucleation and growth contributions, denoted $\dot{f}_n$ and $\dot{f}_g$, respectively:

$$\dot{f} = \dot{f}_n + \dot{f}_g = \frac{f_N}{s_N \sqrt{2\pi}} \exp\left[-\frac{1}{2}\left(\frac{\bar{\varepsilon}^p - \varepsilon_N}{s_N}\right)^2\right]\dot{\bar{\varepsilon}}^p + (1-f)\,\mathrm{tr}(\boldsymbol{D}^p), \tag{5}$$

where $\boldsymbol{D}^p$ is related to Φ_{GTN} by the normality rule:

$$\boldsymbol{D}^p = \dot{\gamma}\frac{\partial \Phi_{GTN}}{\partial \Sigma}. \tag{6}$$

- The expression of the flow stress $\bar{\sigma}$ of the fully dense matrix, which is defined by the Swift law:

$$\bar{\sigma} = K\left(\varepsilon_0 + \bar{\varepsilon}^p\right)^n. \tag{7}$$

- The equivalence between the rates of macroscopic and microscopic (matrix) plastic work:

$$(1-f)\,\overline{\sigma}\,\dot{\overline{\varepsilon}}^p = \boldsymbol{\Sigma} : \boldsymbol{D}^p .$$ (8)

3. Bifurcation approach

The bifurcation theory (see, e.g., Rice, 1976) is used to predict the onset of plastic strain localization in the studied sheet metals. In this approach, bifurcation should be interpreted as the occurrence of a nonhomogeneous strain mode, in the form of an infinite localization band defined by its normal $\vec{n}$, within a continuous medium that is subjected to a homogeneous strain state. Making use of the equilibrium and compatibility conditions, it is possible to derive the following localization criterion, namely the singularity of the acoustic tensor, which only involves the normal $\vec{n}$ to the localization band and the analytical tangent modulus $\boldsymbol{L}$:

$$\det\left(\vec{n}.\boldsymbol{L}.\vec{n}\right) = 0 .$$ (9)

The analytical tangent modulus $\boldsymbol{L}$ is related to the elastic-plastic tangent modulus $\boldsymbol{C}^{ep}$ by:

$$\boldsymbol{L} = \boldsymbol{C}^{ep} + \boldsymbol{C}_1 - \boldsymbol{C}_2 - \boldsymbol{C}_3 ,$$ (10)

where $\boldsymbol{C}_1$, $\boldsymbol{C}_2$ and $\boldsymbol{C}_3$ are fourth-order tensors that can be expressed, after some mathematical derivations, as:

$$C_{1ijkl} = \Sigma_{ij}\,\delta_{kl} \quad ; \quad C_{2ijkl} = \frac{1}{2}\left(\Sigma_{jl}\,\delta_{ik} + \Sigma_{jk}\,\delta_{il}\right) \quad ; \quad C_{3ijkl} = \frac{1}{2}\left(\Sigma_{ik}\,\delta_{jl} - \Sigma_{il}\,\delta_{jk}\right).$$ (11)

The elastic-plastic tangent modulus $\boldsymbol{C}^{ep}$ is determined by expressing the improved GTN yield function and the plastic multiplier in the Kuhn–Tucker form as follows:

$$\Phi_{GTN} \leq 0 \quad ; \quad \dot{\gamma} \geq 0 \quad ; \quad \Phi_{GTN}\,\dot{\gamma} = 0.$$ (12)

This form is convenient because it reveals that there is no plastic flow (i.e., $\dot{\gamma}=0$) when $\Phi_{GTN} < 0$, while a strict plastic loading (i.e., $\dot{\gamma}>0$) necessarily implies that $\Phi_{GTN}=0$ and $\dot{\Phi}_{GTN}=0$. The latter represents the consistency condition, and can be developed as follows:

$$\dot{\Phi}_{GTN} = \boldsymbol{V}_{\Sigma} : \dot{\boldsymbol{\Sigma}} + V_{\overline{\sigma}}\,\dot{\overline{\sigma}} + V_{f^*}\,\dot{f}^* = 0 .$$ (13)

The derivatives $\boldsymbol{V}_{\Sigma}$, $V_{\overline{\sigma}}$ and V_{f^*} are obtained analytically in the following forms:

$$\boldsymbol{V}_{\Sigma} = \frac{2}{\overline{\sigma}}\left(\frac{\boldsymbol{H}:\boldsymbol{\Sigma}}{\overline{\sigma}} + \frac{q_1\,q_2\,f^*}{\kappa}\sinh\left(\frac{3q_2\,\Sigma_m}{\kappa\,\overline{\sigma}}\right)\boldsymbol{I}\right) \quad ; \quad V_{\overline{\sigma}} = -\frac{2}{\overline{\sigma}}\left(\left(\frac{q}{\overline{\sigma}}\right)^2 + 3\frac{q_1\,q_2\,f^*\,\Sigma_m}{\kappa\,\overline{\sigma}}\sinh\left(\frac{3q_2\,\Sigma_m}{\kappa\,\overline{\sigma}}\right)\right)$$

$$V_{f^*} = 2\left(q_1\cosh\left(\frac{3q_2\,\Sigma_m}{\kappa\,\overline{\sigma}}\right) - q_3\,f^*\right).$$ (14)

The rate form of the hypo-elastic law allows us to express the stress rate in terms of the plastic multiplier $\dot{\gamma}$:

$$\dot{\boldsymbol{\Sigma}} = \boldsymbol{C}^e : \left(\boldsymbol{D} - \dot{\gamma} V_\Sigma \right) = \boldsymbol{C}^{ep} : \boldsymbol{D} \,. \tag{15}$$

After some mathematical derivations involving the normality rule (6) and Eqs. (13-15), the elastic-plastic tangent modulus is obtained as follows:

$$\boldsymbol{C}^{ep} = \boldsymbol{C}^e - \frac{\left(\boldsymbol{C}^e : V_\Sigma \right) \otimes \left(V_\Sigma : \boldsymbol{C}^e \right)}{H_\gamma} \,, \tag{16}$$

where H_γ is defined by the following relation:

$$H_\gamma = V_\Sigma : \boldsymbol{C}^e : V_\Sigma - \frac{V_{\bar{\sigma}} \dfrac{\partial \bar{\sigma}}{\partial \bar{\varepsilon}^p}}{(1-f)} \frac{\boldsymbol{\Sigma} : V_\Sigma}{\bar{\sigma}} - V_{f^*} \, \delta_{GTN} \left(\frac{A_n}{(1-f)} \frac{\boldsymbol{\Sigma} : V_\Sigma}{\bar{\sigma}} + (1-f) V_\Sigma : \boldsymbol{I} \right). \tag{17}$$

4. Results and discussion

The constitutive equations of the improved GTN model are numerically integrated, using a fully implicit time integration scheme (Ben Bettaieb et al., 2011), and implemented into the ABAQUS finite element (FE) code via a user material subroutine UMAT. To predict the ductility limits, the bifurcation condition (9) is combined with the above constitutive equations and checked at every time increment. In practice, localized necking is predicted when this condition of singularity of the acoustic tensor is verified. The material parameters of the GTN model and of the hardening law are those adopted for an AA5182 sheet metal according to Mansouri et al. (2014). These parameters are summarized in Table 1.

Table 1. Values for GTN material parameters.

E [GPa]	v	n	K (MPa)	ε_0	f_0	f_c	f_F	q_1	q_2	q_3	s_N	ε_N	f_N
70	0.33	0.17	371.2	0.00324	10^{-3}	0.00213	0.15	1.5	1	2.15	0.1	0.27	0.035

A sensitivity analysis is performed to investigate the effect of the Lankford coefficient r_0 on the ductility limits. In this parametric study, three different sets of Lankford coefficients are considered. The first set, referred to as Set 1, assumes isotropic behavior for the AA5182 material. In order to emphasize the effect of r_0 on the ductility limits, this r_0 Lankford coefficient is varied by setting its value to 1.4 and 0.7, which correspond to Set 2 and Set 3 respectively, as shown in Table 2.

Table 2. Selected sets of Lankford coefficients associated with Hill'48 quadratic yield criterion.

Lankford coefficients	r_0	r_{45}	r_{90}
Set 1 (isotropic)	1	1	1
Set 2	1.4	1	1
Set 3	0.7	1	1

Fig. 1(a) shows the evolution of the analytical tangent modulus component L_{1111} for the different sets of Lankford coefficient r_0, in the case of equibiaxial tensile loading path. The observed trends for the evolution of L_{1111} are quite similar until a value of 0.05 for the macroscopic strain component E_{11}, which corresponds to the onset of coalescence. Starting from this strain threshold, a rapid drop of the stiffness occurs, and differences are evidenced gradually between the isotropic profile and the others. Fig. 1(b) shows the evolution of the minimum of the determinant of the acoustic tensor, $\min(\det(\vec{\boldsymbol{n}}.\boldsymbol{L}.\vec{\boldsymbol{n}}))$, with respect to the logarithmic longitudinal strain for equibiaxial tensile loading path. This function, denoted $\min(\det(\vec{\boldsymbol{n}}.\boldsymbol{L}.\vec{\boldsymbol{n}}))$, represents the minimum of the

determinant of the acoustic tensor over all possible orientations for the normal $\vec{n}$ to the localization band, and it illustrates the evolution of the bifurcation indicator until strain localization is detected. Hence, earlier strain localization is recorded for the largest Lankford coefficient r_0, due to premature void coalescence. To confirm this trend, further simulations are performed for the whole range of strain paths, and the corresponding FLDs are plotted for the different sets of Lankford coefficients considered.
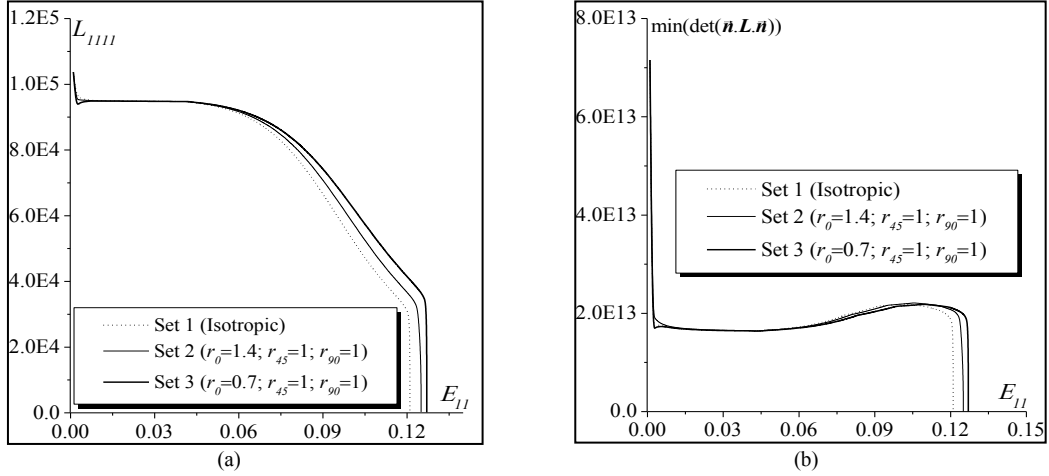

Fig. 1. Prediction of strain localization during equibiaxial tensile loading path. (a) Component L_{1111} with the longitudinal strain E_{11}. (b) Evolution of the minimum of the determinant of the acoustic tensor with the longitudinal strain E_{11}.

Fig. 2(a) reveals, through plots of complete associated FLDs, a strong dependence of the ductility limit on the Lankford coefficient r_0. These observed effects of plastic anisotropy are more significant for negative strain paths. By contrast, they are less pronounced for plane strain and equibiaxial tension, although still noticeable. As has been shown previously, the initiation of strain localization is strongly dependent on the void volume fraction f, through the expression of the analytical tangent modulus L (see Eqs. (10)–(17)). The evolution of the porosity f depends in turn on the Lankford coefficients, as expected and demonstrated in Fig. 2(b). This explains the sensitivity of the shape and the level of the predicted FLDs to the plastic anisotropy.
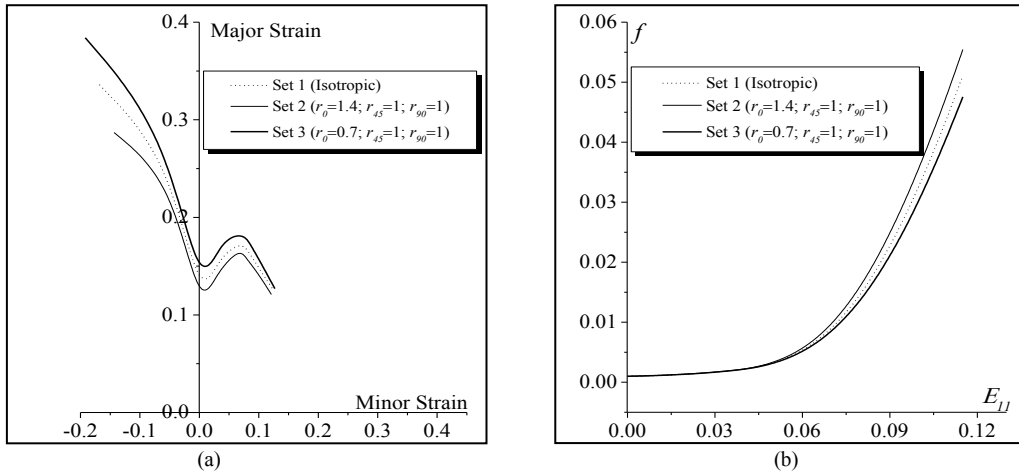

Fig. 2. (a) FLDs obtained for linear strain paths applied along the rolling direction, and (b) evolution of the volume fraction of voids for different values of Lankford coefficient r_0 for the case of equibiaxial tensile state.

Conclusions

An extended GTN model accounting for plastic anisotropy effects has been numerically integrated, using an implicit time integration scheme, and successfully implemented into the FE code ABAQUS. In order to predict FLDs for sheet metals under in-plane biaxial stretching, the current version of GTN model has been coupled with the bifurcation approach. The predicted FLDs show a strong dependence to the Lankford coefficient r_0, especially in the negative strain-path range. Less pronounced, but still noticeable effects on the ductility limits are observed in the positive strain-path range, suggesting different damage behavior depending on the variation of r_0. These findings indicate that the predicted ductility limits may be quite different for a given loading path, depending on the values of Lankford coefficients. For anisotropic sheet metals, it is well known that the consideration of the effect of plastic anisotropy on the ductility limits is crucial in order to determine the actual conditions of strain localization and subsequent failure.

References

Barlat, F., 1987. Crystallographic Texture, Anisotropic Yield Surfaces and Forming Limits of Sheet Metals. Materials Science and Engineering: A 91, 55–72.

Ben Bettaieb, M., Lemoine, X., Duchêne, L., Habraken, A. M., 2011. On the numerical integration of an advanced Gurson model. International journal for numerical methods in engineering 85, 1049–1072.

Benzerga, A. A., Besson, J., 2001. Plastic potentials for anisotropic porous solids. European Journal of Mechanics—A/Solids 20, 397–434.

Butuc, M. C., Da Rocha, A. B., Gracio, J. J., Duarte, J. F., 2002. A more general model for forming limit diagrams prediction. Journal of materials processing technology 125, 213–218.

Cao, J., Yao, H., Karafillis, A., Boyce, M. C., 2000. Prediction of localized thinning in sheet metal using a general anisotropic yield criterion. International Journal of Plasticity 16, 1105–1129.

Franz, G., Abed-Meraim, F., Berveiller, M., 2013. Strain localization analysis for single crystals and polycrystals: Towards microstructure–ductility linkage. International Journal of Plasticity 48, 1–33.

Haddag, B., Abed-Meraim, F., Balan, T., 2009. Strain localization analysis using a large deformation anisotropic elastic–plastic model coupled with damage. International Journal of Plasticity 25, 1970–1996.

Hill, R., 1952. On discontinuous plastic states, with special reference to localized necking in thin sheets. Journal of the Mechanics and Physics of Solids 1, 19–30.

Jaamialahmadi, A., Kadkhodayan, M., 2011. An Investigation Into the Prediction of Forming Limit Diagrams for Normal Anisotropic Material Based on Bifurcation Analysis. Journal of Applied Mechanics 78, 031006.

Karafillis, A. P., Boyce, M. C., 1993. A general anisotropic yield criterion using bounds and a transformation weighting tensor. Journal of the Mechanics and Physics of Solids 41, 1859–1886.

Keeler, S. P., Backofen, W. A., 1963. Plastic instability and fracture in sheets stretched over rigid punches. Asm Trans Q 56, 25–48.

Kim, K. J., Kim, D., Choi, S. H., Chung, K., Shin, K. S., Barlat, F., Youn, J. R. 2003. Formability of AA5182/polypropylene/AA5182 sandwich sheets. Journal of Materials Processing Technology 139, 1–7.

Mansouri, L. Z., Chalal, H., Abed-Meraim, F., 2014. Ductility limit prediction using a GTN damage model coupled with localization bifurcation analysis. Mechanics of Materials 76, 64–92.

Marciniak, Z., Kuczynski, K., 1967. Limit strains in the process of stretch forming sheet metal. International Journal of Mechanical Sciences 9, 609–620.

Rice, J.R., 1976. The localization of plastic deformation. In: Koiter (Ed.), Theoretical and Applied Mechanics, 207–227.

Stören, S., Rice, J. R., 1975. Localized necking in thin sheets. Journal of the Mechanics and Physics of Solids 23, 421–441.

Tvergaard, V., Needleman, A., 1984. Analysis of the cup-cone fracture in a round tensile bar. Acta metallurgica 32, 157–169.